Compensation of Discontinuities in Planar Transmission Lines

RAKESH CHADHA, MEMBER, IEEE, AND K. C. GUPTA, SENIOR MEMBER, IEEE

Abstract —Compensation of discontinuity reactances associated with steps, right-angled bends, and T-junctions in planar transmission lines has been carried out by removing appropriate triangular portions from the discontinuity configurations. A two-dimensional analysis using a Green's functions approach has been employed.

I. Introduction

PLANAR TRANSMISSION lines (such as stripline, microstrip line, suspended-substrate stripline, inverted microstrip, etc.) are used in the design of microwave and millimeter-wave circuits. Geometrical discontinuities associated with these lines affect the circuit performance. It is thus desirable to reduce the effects of discontinuity reactances. Steps, bends, and T-junctions are some of the commonly occuring discontinuities. Compensation of discontinuity reactances for the steps occuring in stripline transformers and filters has been presented [1]. Douville and James [2] have carried out experimental study of symmetrical microstrip bends and their compensation has been attempted by chamfering the bend. Compensation of T-junctions in striplines and microstrip lines has been reported [3]–[6]. In the compensation proposed by Dydyk [3], strip widths are altered near the junction. The analysis ignores the reactances caused by the steps thus introduced. Also, this method is not very effective over a wide range of frequencies. The other methods [4]–[6] alter the junction to a Y-junction and the branch line is no longer perpendicular to the main line. In some cases, this may be undesirable as it may necessitate introducing bends in layout, etc. In this paper, methods of compensation of reactances in steps, right-angled bends, and T-junctions in planar waveguides are reported. These results can be used for the planar transmission lines for which planar waveguide models are available. Various dimensions considered correspond to those of the planar models. Widths shown in various figures, are effective widths for microstrip configurations.

Two-dimensional (2-D) analysis [7]–[9] is used to analyze accurately the discontinuities without and with the proposed compensations. The 2-D analysis is based upon Green's functions [10], [11] and the segmentation [8], [10] and desegmentation [6], [9] methods. Details of this method of analysis as well as its limitations have been discussed in literature [6], [8], [9], [11] earlier.

Manuscript received March 10, 1982; revised June 28, 1982.

R. Chadha was with the Department of Electrical Engineering, Indian Institute of Technology, Kanpur, India. He is now with the Department of Electrical Engineering, University of Waterloo, Waterloo, Ont., Canada, N2L 3G1.

K. C. Gupta is presently with the Department of Electrical Engineering, University of Kansas, Lawrence, KS 66045, on leave from the Department of Electrical Engineering, Indian Institute of Technology, Kanpur 208016, India.

II. Steps in Width

A step discontinuity is present in impedance transformers, half-wave filters, or wherever a change in impedance is involved. Compensation of steps used in stripline transformers and filters has been reported earlier [1]. A one-dimensional analysis is used in [1] and the compensation achieved is not broad band. In this section, compensation of steps with impedance ratios $1:2$ and $1:\sqrt{2}$ has been attempted by chamfering the corners so that the width does not change abruptly.

Fig. 1 (inset) shows a symmetrical step in width (impedance ratio $1:2$) of the line. The discontinuity reactances cause the reflection coefficients on the two sides of the step to be different from their theoretical values of $\pm 1/3$ (at the plane of the step). The magnitude of the reflection coefficient is shown as a function of frequency in Fig. 1 (curve for $\theta = 90°$). The phases of the reflection coefficients are used to obtain the locations of the effective step reference planes, i.e., where S_{11}, S_{22} become real. The normalized electrical lengths Δl_i between the step plane and the effective step reference planes are plotted in Fig. 2. Δl_i is the distance between the step reference plane from the magnetic wall model of the line and the effective step plane computed from S_{ii}. It is taken to be positive if the effective reference plane shifts away from port i and negative if the effective reference plane shifts towards port i. It is desired that the normalized electrical lengths Δl_i either be small or remain constant with frequency and that the magnitude of reflection coefficient be close to $1/3$.

To reduce the effects of the discontinuity reactances, the step is chamfered so that the width varies in a tapered manner as shown in the insert in Fig. 1. The desegmentation method [9] is used to analyze chamfered steps with three values of θ, 30°, 45°, and 60°. Variations of the magnitudes of the reflection coefficients for these three chamfered steps are shown as functions of frequency in Fig. 1. The corresponding normalized electrical lengths for the chamfered steps are shown as functions of frequency in Fig. 2. In these cases, the step plane is considered midway in the taper and the shift to the equivalent step reference

0018-9480/82/1200-2151$00.75 ©1982 IEEE

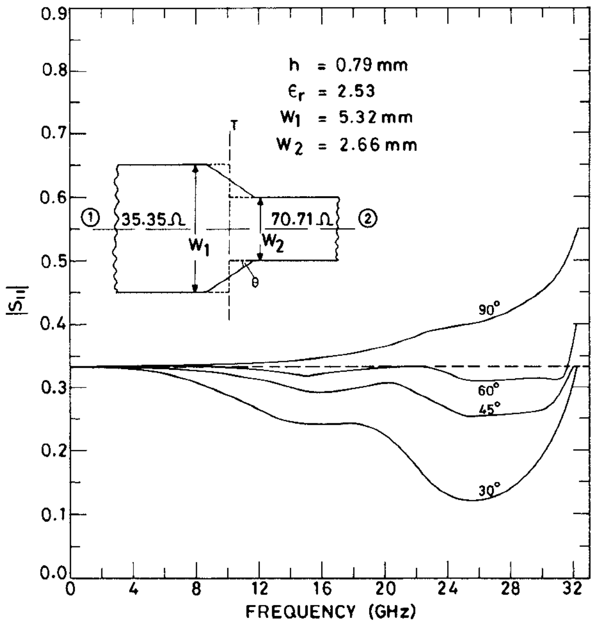

Fig. 1. Reflection coefficients for uncompensated and compensated step discontinuities with a 1 : 2 impedance ratio.

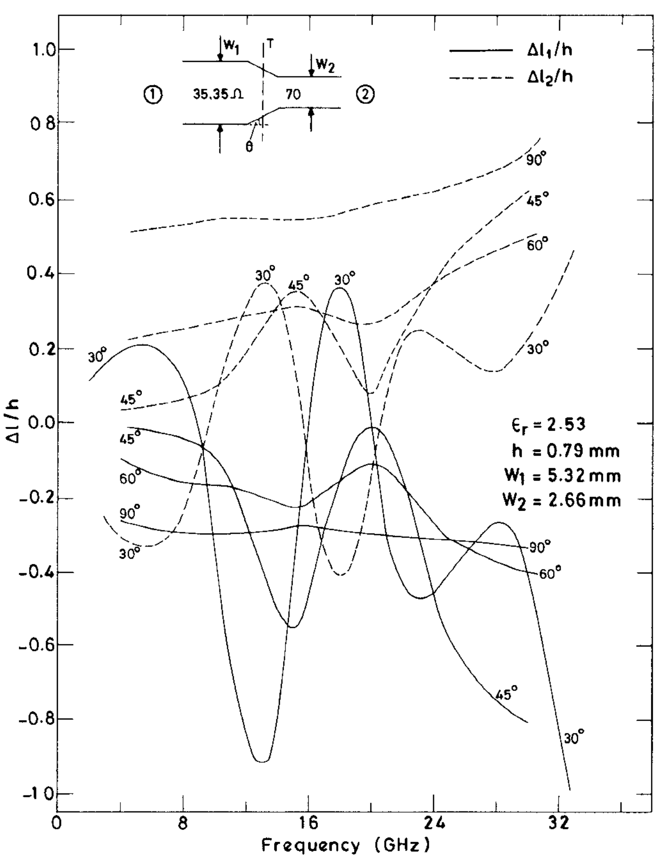

Fig. 2. Normalized shift in the effective step reference planes for the uncompensated and compensated step discontinuities with a 1 : 2 impedance ratio.

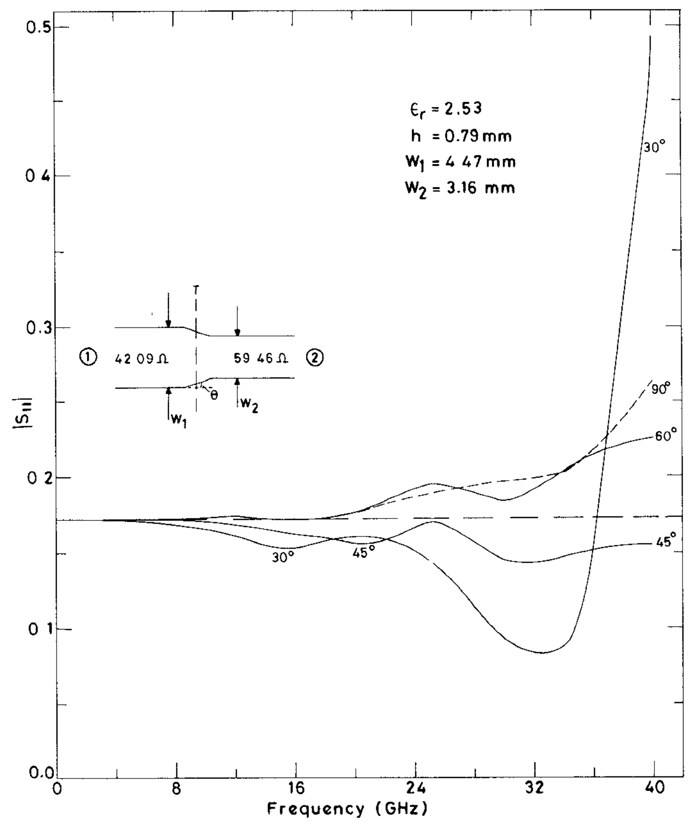

Fig. 3. Reflection coefficients for uncompensated and compensated step discontinuities with a $1:\sqrt{2}$ impedance ratio.

planes is plotted in terms of normalized electrical length. It is seen that the performance of a chamfered step with $\theta = 60°$ is closest to the ideal behavior.

It may be noted that for the case considered in Fig. 1, cutoff frequency for the first higher order (TE_{10}) mode in the wider line is 17.723 GHz. However, for the TEM-mode input, the TE_{10} mode would not be excited because of the symmetry in the step. However, the next higher mode (TE_{20} with a cutoff of 35.445 GHz) would be excited in this case. In Fig. 1, the increase in $|S_{11}|$ seen near 32 GHz is related to the proximity of the cutoff of the TE_{20} mode.

A symmetrical step with an impedance ratio of $1:\sqrt{2}$ has also been considered. Unchamfered ($\theta = 90°$) and chamfered steps (with θ equal to 30°, 45°, and 60°) have been analyzed. The magnitudes of the reflection coefficients in the four cases are plotted as functions of frequency in Fig. 3. The desired magnitude of the reflection coefficient is 0.172. The normalized electrical lengths corresponding to the separation between the step plane (midway in the taper) and the equivalent step reference planes (computed from S_{ii}) are plotted for the four cases in Fig. 4. In this case also, 60° taper may be chosen for a performance closest to the ideal behavior, especially when the shift in the reference plane of the step is considered.

In both of the examples considered, it is seen that for $\theta = 45°$, 60°, or 90°, Δl_1 is negative and Δl_2 is positive. The S_{11} and S_{22} become real at planes which are shifted towards the line of greater width. It may be noted that this shift is from the magnetic wall model and is much smaller than the shift towards the line of smaller width which is involved in obtaining the magnetic wall model from the physical dimensions.

The results for the symmetrical steps discussed above also correspond to their even-mode half-sections (unsym-

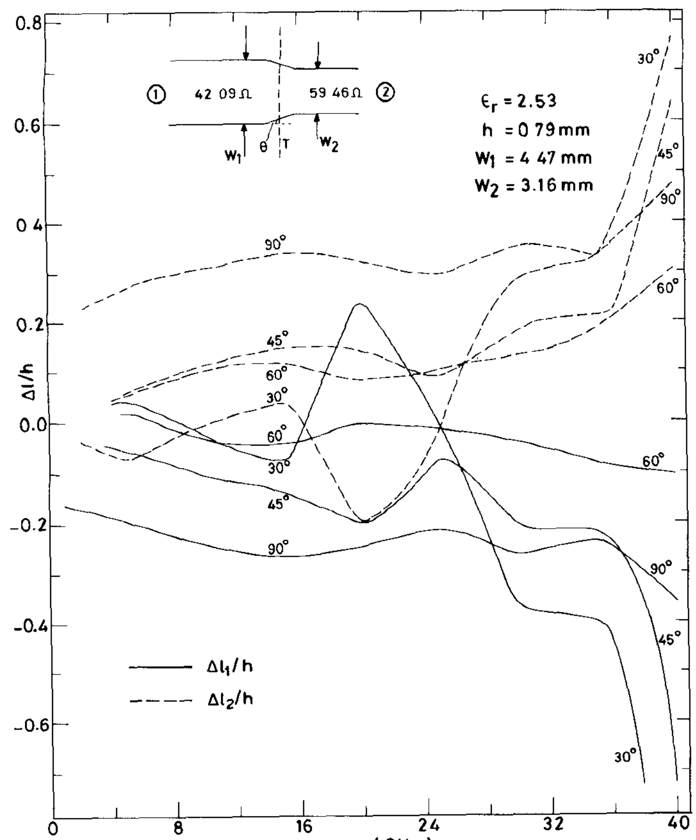

Fig. 4. Normalized shift in the effective step reference planes for the uncompensated and compensated step discontinuities with a $1:\sqrt{2}$ impedance ratio.

metrical step with half the line widths). Chamfering could also be used for steps with other impedance ratios.

III. Right-Angled Bends

Compensation of right-angled microstrip bends has been obtained experimentally by chamfering the corner [2]. However, no analytical results have been reported so far. In this section, theoretical results are presented for a right-angled bend in planar waveguides. It is seen that the percentage of chamfer required remains constant, independent of dielectric constant, width, etc.

Variation in reflection coefficient for an unchamfered right-angled bend is shown in Fig. 5. The high values of $|S_{11}|$ above 25 GHz are related to the next higher mode cutoff at 30.607 GHz. To reduce the effect of the discontinuity reactances, a right-angled triangular portion can be removed from the corner. As the line widths on the two sides of the bend are equal, symmetry suggests that the chamfer be an isosceles triangle. The size of the triangle removed has been optimized, so that the magnitude of the reflection coefficient is minimum. The optimum value of the smaller sides of the triangle equals 0.828 times the width W. This is independent of all other parameters and it makes the distance from the inner corner to the opposite chopped edge also equal to $0.828W$. The variation of reflection coefficient for an optimally chamfered bend is also shown in Fig. 5.

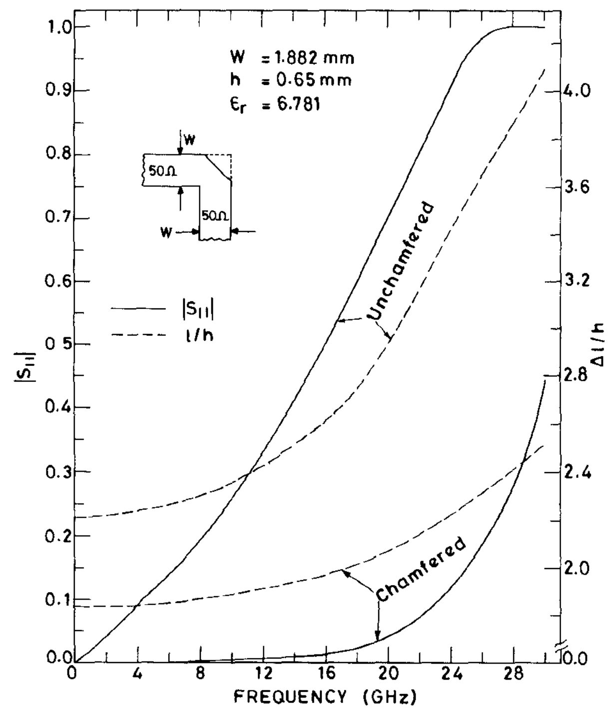

Fig. 5. Reflection coefficients and normalized electrical lengths for uncompensated and optimally compensated right-angled bends.

The equivalent electrical length for the bend can be computed from the transmission coefficient. The normalized electrical length between two planes of the bend for the unchamfered and the chamfered bends has also been plotted in Fig. 5. It is seen that the normalized electrical length for the chamfered bend varies only slightly whereas the normalized length for the unchamfered bend varies significantly.

Even though the percentage chamfering required in planar waveguide model has a constant value, it changes when the physical dimensions of a stripline or a microstrip bend are being considered. This happens because the distance between the magnetic wall and the physical periphery is not proportional to the width. The percentage chamfering needed (in physical dimensions) would decrease on increasing the width-to-height ratio.

If the two lines joined at the bend are of unequal widths, the discontinuity effects would still get reduced by removing a right-angle triangle. In such cases, the line with the wider width should be chopped more than the line of smaller width.

IV. T-Junctions

Discontinuity reactances associated with a T-junction can be compensated by removing a triangular portion from the junction as shown in the Fig. 6 inset. In this section, two symmetric T-junctions with branch line impedances either equal to the main line impedance or $1/\sqrt{2}$ of the main line impedance are considered. These T-junctions are used frequently in stubs, SPDT switches, hybrids, power dividers, couplers, etc.

The magnitudes of the reflection coefficients at the branch line and at the main line for the $1/\sqrt{2}:1:1$ T-junc-

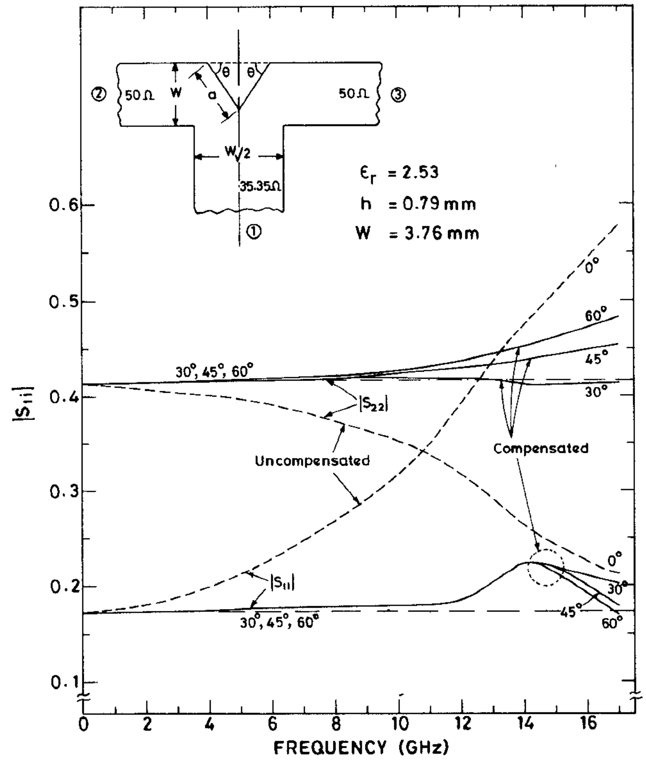

Fig. 6. Main line and branch line reflection coefficients for uncompensated and compensated T-junctions (impedance ratio $1/\sqrt{2}:1:1$).

tion are shown as functions of frequency in Fig. 6.

As in the case of a step discontinuity, the phases of the reflection coefficients are used to obtain the locations of the effective junction reference planes where S_{11}, S_{22} become real. The shifts Δl_t in the effective junction planes are taken as follows. For the branch port the shift is taken from the plane where the branch line joins the main line (plane T_1 in Fig. 7) and for the ports on the main line the shift is from the plane midway between the two ports on the main line (plane T_2 in Fig. 7). The normalized electrical lengths representing these shifts are plotted in Fig. 7 for ports 1 and 2. The positive and negative signs for Δl_t are taken in the same manner as for the step discontinuity.

For compensation of discontinuity reactances, the removal of isosceles triangles with the angle θ equal to 30°, 45°, and 60° has been considered. The sides "a" of the isosceles triangles removed have been optimized for each of the three values of θ. In optimization, the deviations of the magnitudes of the branch line and the main line reflection coefficients from their ideal values (0.172 and 0.414, respectively) are minimized. The optimum values of "a" are $0.851W$, $0.807W$, and $0.879W$ for θ values equal to 30°, 45°, and 60°, respectively. The variations of the magnitudes of reflection coefficients at the branch line and the main line for the optimized junctions are shown in Fig. 6 for different values of θ. Normalized electrical lengths representing the shifts in the junction planes are plotted in Fig. 7. It is seen that by chopping off an isosceles triangle with $\theta = 30°$ the effects of discontinuity reactances are minimized.

Equi-impedance T-junctions (1:1:1) have also been considered for compensation. Sides "a" of the isosceles

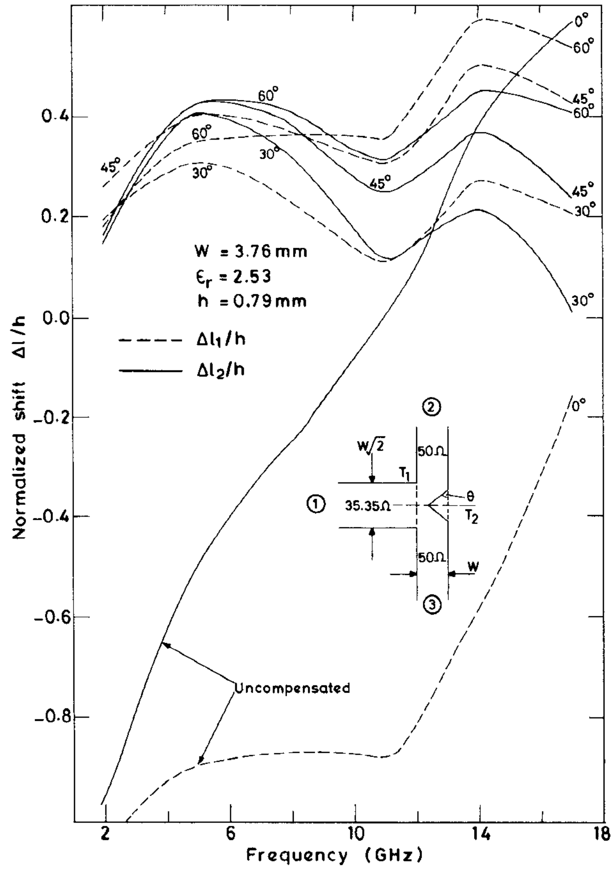

Fig. 7. Normalized shift in the effective junction planes for the uncompensated and compensated T-junctions (impedance ratio $1/\sqrt{2}:1:1$).

triangles to be removed have again been optimized for the same three values of θ. The deviations of magnitudes of S_{11} and S_{22} from the ideal value of 1/3 are minimized. The optimum values of "a" are $0.601W$, $0.569W$, and $0.666W$ for θ values equal to 30°, 45°, and 60°, respectively. The variations of the magnitudes of the reflection coefficients for the uncompensated and compensated junctions are shown in Fig. 8. Normalized electrical lengths representing the shift in the junction planes are plotted in Fig. 9 for the uncompensated and compensated junctions. In this case, the discontinuity reactances are again minimized by removing an isosceles triangle with $\theta = 30°$.

In optimizing the performance of the junctions, the side of the triangle is chosen such that the magnitudes of the reflection coefficients at ports 1 and 2 are close to their ideal values (giving equal weights to both the deviations). A least-square optimization procedure has been employed. The side of the triangle chopped off would be different for different values of relative weightings given to the deviations in the two reflection coefficients.

The side of the triangle to be removed is found to vary with the frequency at which optimization is carried out. However, this variation is quite small. In the results discussed above, optimization is carried out at two spot frequencies and the mean value is considered for "a". For the case of equi-impedance T-junction, optimum values of a/W (with $\theta = 45°$) at 8 GHz and at 15 GHz are 0.544 and 0.594, respectively. Also, it is observed that for a given Z_0 and height of the substrate, the ratio of optimum side of

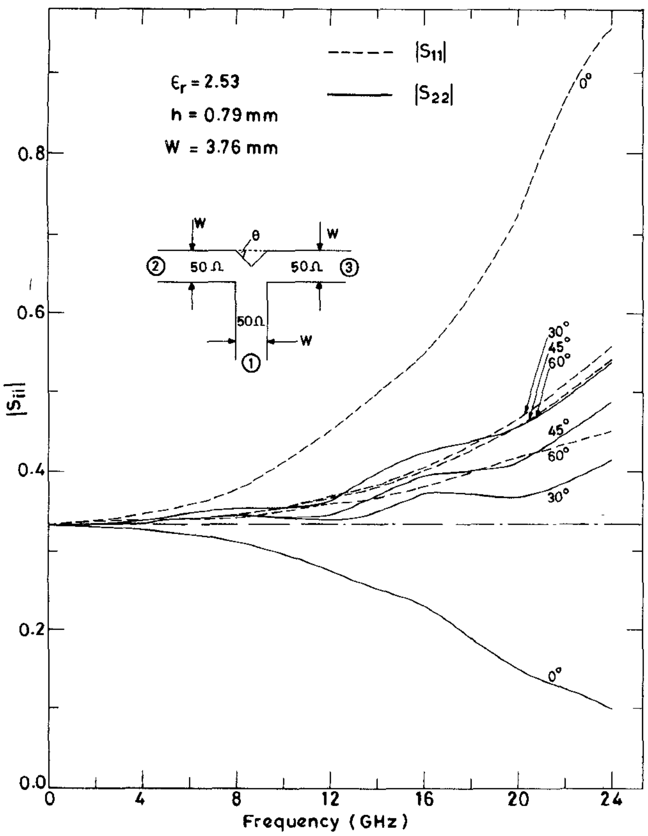

Fig. 8. Main line and branch line reflection coefficients for uncompensated and compensated T-junctions (impedance ratio 1 : 1 : 1).

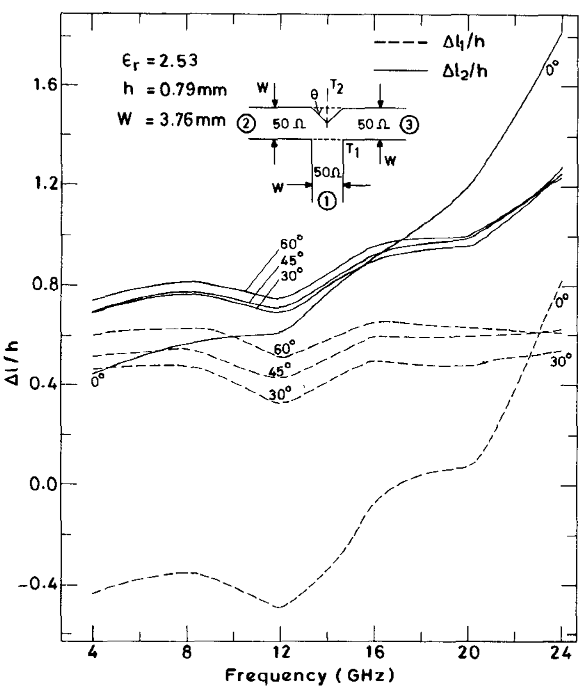

Fig. 9. Normalized shift in the effective junction planes for the uncompensated and compensated T-junctions (impedance ratio 1 : 1 : 1).

the triangle to be removed to the width of the line is independent of the dielectric constant of substrate. Thus if the frequency dependence of the optimum side "a" is ignored, the optimum value of the ratio a/W is independent of all other parameters.

By considering a plane of symmetry located half way through the width of the branch line, the T-junction can be compared with a right-angled bend on one side of this plane. The reflection coefficient at the branch line of the T-junction is equal to that at the corresponding side of the bend. Thus, if only the branch line reflection coefficient is to be optimized, only a right-angled bend need be considered. In such a case, the results discussed in Section III also correspond to a T-junction with branch line impedance equal to one half of the main line impedance.

V. Concluding Remarks

Compensation of discontinuity reactances caused by steps, right-angled bends, and T-junctions in planar waveguides has been discussed. These results can be applied directly to the planar transmission lines for which the outward extension of the periphery to obtain the equivalent magnetic wall model is known. Thus, the results presented should find applications in the design of MIC's using such planar transmission lines.

The compensation has been carried out by removing appropriate triangular portions from the discontinuity configurations. This technique can be used for compensation of other types of discontinuities. The method discussed herein could also be used for compensation of discontinuities in waveguides.

References

[1] K. C. Gupta and R. Chadha, "Design real-world stripline circuits," *Microwaves*, vol. 17, no. 12, pp. 70–80, Dec. 1978.
[2] R. J. P Douville and D. S. James, "Experimental study of symmetric microstrip bends and their compensation," *IEEE Trans. Microwave Theory Tech.*, vol. MTT-26, pp. 175–182, Mar. 1978.
[3] M. Dydyk, "Master the T-junction and sharpen your MIC designs," *Microwaves*, vol. 16, no. 5, pp. 184–186, May 1977.
[4] W. Menzel, "Frequency dependent transmission properties of microstrip Y-junctions and 120°-bends," *Inst. Elec. Eng. J. Microwaves, Opt., Acoust.*, vol. 2, pp. 55–59, 1978.
[5] R. Mehran, "Compensation of microstrip bends and Y-junctions with arbitrary angle," *IEEE Trans. Microwave Theory Tech.*, vol. MTT-26, pp. 400–405, June 1978.
[6] K C. Gupta, R. Chadha, and P. C. Sharma, "Two-dimensional analysis for stripline/microstrip circuits," in *1981 IEEE MTT-S Int. Symp. Dig.*, pp. 504–506, June 1981.
[7] T. Okoshi and T. Miyoshi, "The planar circuit—An approach to microwave integrated circuitry," *IEEE Trans. Microwave Theory Tech.*, vol. MTT-20, pp. 245–252, Apr. 1972.
[8] R. Chadha and K. C. Gupta, "Segmentation method using impedance matrices for the analysis of planar microwave circuits," *IEEE Trans. Microwave Theory Tech.*, vol. MTT-29, pp. 71–74, Jan. 1981.
[9] P. C. Sharma and K. C. Gupta, "Desegmentation method for analysis of two-dimensional microwave circuits," *IEEE Trans. Microwave Theory Tech.*, vol. MTT-29, pp. 1094–1098, Oct. 1981.
[10] T. Okoshi and T. Takeuchi, "Analysis of planar circuits by segmentation method," *Electron. Commun. Japan*, vol. 58-B, no. 8, pp. 71–79, Aug. 1975.
[11] R. Chadha and K. C. Gupta, "Green's functions for triangular segments in planar microwave circuits," *IEEE Trans. Microwave Theory Tech.*, vol. MTT-28, pp. 1139–1143, Oct. 1980.

Rakesh Chadha (S'79–M'81) was born in Udhampur, J&K, India, on November 12, 1955. He received the B. Tech. degree in electrical engineering from the Indian Institute of Technology, Delhi, India, in 1977 and the Ph.D. degree in electrical engineering from the Indian Institute of Technology, Kanpur, India, in 1982.

From September 1977 to February 1982, he was with the Department

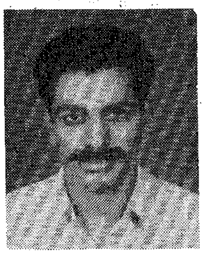

of Electrical Engineering, Indian Institute of Technology, Kanpur, India, working as a Research Engineer in the area of computer-aided analysis and design of microwave integrated circuits. Presently, he is with the Department of Electrical Engineering, University of Waterloo, Waterloo, Ontario, Canada, working in the area of optimization for large networks. He has published ten research papers and is a co-author of the book *Computer-Aided Design of Microwave Circuits*, Artech House, 1981.

K. C. Gupta (M'62–SM'74) was born in 1940. He received the B.E. and M.E. degrees in electrical communication engineering from Indian Institute of Science, Bangalore, India, in 1961 and 1962, respectively, and the Ph.D. degree from Birla Institute of Technology and Science, Pilani, India, in 1969.

He worked at Punjab Engineering College, Chandigarh, India, from 1964 to 1965, the Central Electronics Engineering Research Institute, Pilani, India, from 1965 to 1968, and Birla Institute of Technology from 1968 to 1969. Since 1969 he has been with the Indian Institute of Technology, Kanpur, India, and has been a Professor of electrical engineering since 1975. On leave from the Indian Institute of Technology, he was a Visiting Professor at the University of Waterloo, Canada from 1975 to 1976, Ecole Polytechnique Federale de Lausanne, Switzerland, in 1976, Technical University of Denmark from 1976 to 1977, and Eidgenossische Technische Hochschule, Zurich, Switzerland, in 1979. From 1971 to 1979 he was Coordinator for the Phased Array Radar Group of Advanced Centre for Electronic Systems at the Indian Institute of Technology. He has published four books: *Microwave Integrated Circuits*, Wiley Eastern and Halsted Press, 1974, *Microstrip Lines and Slotlines*, Artech House, 1979, *Microwaves*, Wiley Eastern, 1979 Halsted Press, 1980, and *Computer-Aided Design of Microwave Circuits*, Artech House, 1981. He has published over 70 research papers and holds one patent in microwaves areas.

Dr. Gupta is a fellow of the Institution of Electronics and Telecommunication Engineers (India).

Millimeter-Wave Hybrid Coupled Reflection Amplifiers and Multiplexers

DAVID RUBIN, MEMBER, IEEE

***Abstract*—Multiple stage hybrid coupled reflection amplifiers and frequency multipliers are modeled using two-port analysis. A two-stage (4 diode) microstrip InP Gunn amplifier and a four-section suspended substrate multiplexer were fabricated in *Ka* band. Analysis shows that the performance of the hybrid coupled amplifier, both for packaged diodes and pure negative resistance (ideal monolithic) devices, is extremely sensitive to input and output VSWR's.**

I. Introduction

The 3-dB QUADRATURE coupler is one of the most useful microwave components available to the circuit designer. The amplifier and multiplexer configurations to be described both use the equal power split and 90° phase differences between output terminals of these "hybrids". Symmetry makes it possible to reduce the analysis of the four-port network to that of a two-port. Identical terminations present no problems since they do not upset symmetry and can be considered part of the coupler for analysis purposes. Nonidentical terminations, such as two different diodes, can be handled by signal flow graphs, again reducing the circuit to an equivalent two-port.

This paper describes the analysis of complex microwave circuits which utilize 3-dB quadrature couplers. Both computer results and measurements will be given for: 1) single and multistage hybrid coupled small signal reflection amplifiers, and 2) multichannel hybrid coupled multiplexers.

Predicted behavior of ideal negative resistance devices is also computed for circuits which utilize different practical hybrid couplers and mismatched input and output impedances. It will be shown that small mismatches can lead to large amplitude ripple and input VSWR.

II. Analysis of Cascaded Hybrid Coupled Reflection Amplifiers

All solid-state amplifiers for use above 40 GHz use negative resistance one-port devices as amplifying elements. To separate input and output power, ferrite circulators are normally used. At the higher millimeter-wave frequencies, circulators are bandwidth limited; another technique, that of coupling two identical amplifier stages through 3-dB quadrature couplers, is sometimes used [1]. This method makes use of the fact that the two output

Manuscript received March 16, 1982; revised June 18, 1982.
The author is with Millimeter-Wave Technology Branch, Naval Ocean Systems Center, San Diego, CA 92152.